food & nutrition research

ORIGINAL ARTICLE

Circadian dysregulation disrupts gut microbe-related bile acid metabolism

Rulong Chen, Mengcheng Ruan, Si Chen, Yu Tian, Hualin Wang, Na Li, Junlin Zhang, Xiaoli Yu and Zhiguo Liu*

Hubei Province Engineering Research Center of Healthy Food, School of Biology and Pharmaceutical Engineering, Wuhan Polytechnic University, Wuhan, China

Popular scientific summary

- The normal circadian fluctuations of the CLOCK and REV-ERBα disappeared (normal diet) or were reversed (high-fat diet) in *Per1*/*Per2* double gene knockout mice
- Mice intestinal total BA and conjugated BA were affected by circadian rhythm under both normal and high-fat diets, while these circadian fluctuations disappeared in *Per1*/*Per2* double gene knockout mice.
- Mice intestinal unconjugated BA only affected by diet without obvious fluctuations associated with circadian rhythm.
- The ratio of conjugated/unconjugated BA was positively correlated with the presence of Bacteroidetes and displayed a circadian rhythm.
- Circadian changes to intestinal ratios of conjugated/unconjugated BA have the potential to regulate diurnal fluctuations in liver BA synthesis via FXR-FGF15.

Abstract

***Background*:** Disturbance of circadian rhythm leads to abnormalities in bile acid (BA) and lipid metabolism, and it is of great significance to explore the relationship between them. This study explored the effects of circadian dysregulation on the rhythms of intestinal BA metabolism.
***Method*:** *Period circadian clock 1*/*period circadian clock 2* (*Per1*/*Per2*) double gene knockout (DKO) and wild-type (WT) male C57BL/6 mice were fed with a control or high-fat diet for 16 weeks. We measure plasma parameters of mice. Pathological changes including those in liver and intestine were detected by hematoxylin and eosin (H&E) and oil O staining. Western blot was used to detect the intestinal core rhythm protein clock circadian regulator (CLOCK), nuclear receptor subfamily 1, group D, member 1 (REV-ERBα), Farnesoid X receptor (FXR), Small heterodimer partner (SHP), and Fibroblast growth factor 15 (FGF15) expressions. We analyzed the bile acid and intestinal flora profile in the mice intestine tissues by BA-targeted metabolomics detection and high-throughput sequencing.
***Results*:** Rhythmic chaos affected lipid metabolism and lipid accumulation in mice liver and intestine, and diurnal fluctuations of plasma triglycerides (TGs) were absent in normal-feeding DKO mice. The normal circadian fluctuations of the CLOCK and REV-ERBα observed in wild mice disappeared (normal diet) or were reversed (high-fat diet) in DKO mice. In WT mice intestine, total BA and conjugated BA were affected by circadian rhythm under both normal and high-fat diets, while these circadian fluctuations disappeared in DKO mice. Unconjugated BA seemed to be affected exclusively by diet (significantly increased in the high-fat group) without obvious fluctuations associated with circadian rhythm. Correlation analysis showed that the ratio of conjugated/unconjugated BA was positively correlated with the presence of Bacteroidetes and displayed a circadian rhythm. The expression levels of BA receptor pathway protein FXR, SHP, and FGF15 were affected by the ratio of conjugated/unconjugated BA.
***Conclusion*:** *Bacteroidetes*-related diurnal changes to intestinal ratios of conjugated/unconjugated BA have the potential to regulate diurnal fluctuations in liver BA synthesis via FXR-FGF15. The inverted intestinal circadian rhythm observed in DKO mice fed with a high-fat diet may be an important reason for their abnormal circadian plasma TG rhythms and their susceptibility to lipid metabolism disorders.

Keywords: *high-fat diet*; *circadian rhythm*; *bile acid*; *intestinal flora*

To access the supplementary material, please visit the article landing page

Received: 3 March 2021; Revised: 29 March 2022; Accepted: 21 June 2022; Published: 19 August 2022

Physiological and behavioral circadian rhythms are driven by internal molecular oscillators synchronized with sunrise and sunset, enabling organisms to adapt to an external environment that alternates between day and night (1). The circadian rhythm system consists of two parts: the central clock and the peripheral clock. The central clock is located in the suprachiasmatic nucleus (SCN) of the hypothalamus, is controlled by light/darkness, and synchronously affects metabolic functions. The peripheral clock receives signals from the central clock through hormones and synaptic projections and is affected by the autonomic nervous system as well as by external factors (such as light, sleep, physical activity, feeding, etc.) (2). The circadian rhythm system is closely integrated with energy metabolism through both central and peripheral clocks (3, 4). The master regulators of the circadian clock, Brain and Muscle Aryl Hydrocarbon Receptor Nuclear Translocation 1 (BMAL1 (*Arntl*)) and CLOCK (*Clock*), form heterodimers and combine with E-box elements to regulate the expression of target genes, such as *Per1*/*Per2* and cryptochrome 1/cryptochrome 2 (*Cry1*/*Cry2*). PER1/PER2 and CRY1/CRY2 accumulate in cells and form heterodimers that inhibit *Clock*/*Arntl* transcription (5–7). This feedback system also promotes the transcription of rhythm output factors REV-ERBα (*Nr1d1*) and retinoic acid receptor-related orphan receptor α (RORα (*Nr1f1*)), which can also inhibit or activate the transcription of core rhythm genes (8).

This autonomous cellular clock is expressed in all somatic cells and entrained by the central clock and other regulatory inputs (9). Food composition and eating time are important external influences and affect the fluctuation of rhythm in most tissues (10), in addition to affecting intestinal flora diversity. Studies have demonstrated that intestinal flora is essential for the maintenance of peripheral circadian rhythm (11). Although the underlying mechanism is not clear, short-chain fatty acids and BAs related to intestinal microbial metabolism are important signals that affect circadian rhythm and related metabolic parameters (12). Furthermore, these compounds are also strongly related to metabolic diseases, such as obesity and glucose intolerance (13).

BAs are essential cholesterol-derived nutritional signal molecules, which are synthesized in the liver and can be used as detergents to dissolve dietary lipids (14). In the gallbladder, unconjugated BA is conjugated with taurine or glycine to form conjugated BA (15). After entering the intestine, BA assists the digestion and absorption of lipids and then returns to the liver via the portal vein to complete the intestine-liver loop (16). Conjugated BA can be decomposed into unconjugated BA and further metabolized into secondary BA by intestinal flora (17). Our previous studies on mice bile metabolism showed that the circadian patterns of metabolites involved in primary BA synthesis, fatty acid synthesis, and amino acid metabolism were significantly different between normal and high-fat diets (18). These effects are related to circadian changes of intestinal flora (19), but the relationships between various types of intestinal BAs and their circadian fluctuations remain unclear.

FXR is a major BA receptor, which participates in intestinal glucose and lipid metabolism (20), in addition to inhibiting the synthesis of hepatic BA in the liver via the hormone signal FGF15 (21, 22). Previous studies have shown that circadian dysregulation can cause BA metabolism disorders through different mechanisms: disruption of the circadian rhythm of liver BA synthesis (23), obstruction of liver-intestinal BA transport by disrupting the circadian rhythm of BA transporters (24), and/or modifying the circadian rhythm of intestinal flora (25). Studies have also found that *Per1*/*Per2*$^{-/-}$ mice are characterized by liver BA loss of homeostasis and activation of both xenobiotic receptor constitutive androstane (CAR) and pregnane X receptors (PXRs), leading to cholestatic disease (26). These studies suggest that the circadian rhythm of BA synthesis and metabolism plays an important role in intestinal lipid absorption metabolism and is related to a variety of metabolic abnormalities. However, many details are currently clear and require further study.

In this study, we used *Per1*/*Per2*$^{-/-}$ mice to observe the effects of circadian clock defects on intestinal BA, intestinal flora, and BA regulatory proteins under both normal and high-fat diets, gaining insight into the relationship between circadian rhythm and intestinal BA metabolism.

Materials and methods

Animals and diets

This animal study was conducted according to the Guidelines for the Care and Use of Experimental Animals, and the protocol was approved by the Laboratory Animal Ethics Committee of Wuhan Polytechnic University (ID Number: 20160709003). *Per1*$^{-/-}$/*Per2*$^{-/-}$ mice from Soochow University were used as a research model for the disappearance of circadian rhythm (27). The wild-type male C57BL/6 mice (7 weeks old, weighing 18–20 g) were purchased from the Center for Disease Control of Hubei Province (Wuhan, China). Mice were acclimatized to cleaning laboratory conditions for 1 week. Mice were provided free access to food and water and were housed under a 12 h day/night cycle with a room temperature of 22 ± 1°C and relative humidity of 60 ± 5%. Mice were randomly allocated to four groups (20 animals per group), and each group was fed one of two diets for 16 weeks. Wild-type control mice (WTCON group) and *Per1*/*Per2* double knockout mice (DKOCON group) were fed with a normal chow diet with 10 kcal% fat (formulated according

Citation: Food & Nutrition Research 2022, **66**: 7653 - http://dx.doi.org/10.29219/fnr.v66.7653

to NIH-41 standards developed by the National Institutes of Health). High-fat diet-fed wild-type mice (WTHFD group) and double knockout mice (DKOHFD group) were fed with a high-fat diet with 42 kcal% fat and 0.5% cholesterol (w/w) (formulated according to Hayek Western Diet Model Feed). All feed components were purchased from Trophic Animal Feed High-Tech Co., Ltd, China. Detailed information regarding these diets is presented in Supplementary Table 1.

Three mice were housed in each cage. Each week, the body weight of each mouse was measured. At the 16th week of the experiment, animals were randomly divided into two time point groups: ZT0 (7:00 am, n = 10) and ZT12 (7:00 pm, n = 10). Mice were then sacrificed at these two time points (ZT0 and ZT12). Mice in each group stopped eating 12 h before execution. Orbital blood was gathered into a heparinized tube (1.5 mL) and centrifuged at 1,000× g for 15 min at 4 °C. Plasma was collected and stored at −80 °C until analysis. Concurrently, the liver and fat of each mouse were weighed and recorded. Liver weight/body weight and fat weight/body weight ratios were calculated according to liver weight, fat weight, and body weight. Liver and small intestine tissues were rinsed with 0.9% sodium chloride solution and weighed; after which they were stored at −80°C.

Measurement of plasma parameters

Bile acids are related to the absorption and metabolism of cholesterol and triglycerides. Therefore, this study observed the diurnal changes of total cholesterol (TC) and triglycerides (TG) in blood. The plasma total cholesterol and triacylglycerol were determined using kits according to the manufacturer's instructions (Nanjing Jiancheng Bioengineering Institution, Nanjing, China).

Histological studies

The liver and intestine are the main organs of bile acid synthesis and metabolism, which regulate glucose and lipid metabolism through the intestinal-liver circulation of bile acids. The liver tissue samples were taken from the central part of the largest lobe. Intestinal tissue samples were taken from the lower segment of the small intestine. Fixed liver and intestine tissues were dehydrated, embedded in paraffin, and sectioned with 10% paraformaldehyde solution for 24 h. Sections were dewaxed using xylene, and intestinal tissues were stained with hematoxylin and eosin (H&E) or Masson's trichrome. Liver tissues were stained with Oil red O.

Small intestine BA-targeted metabolomics detection

There are many kinds of bile acids, which are usually detected qualitatively and quantitatively by targeted metabolome. The pretreatment method for BA samples was provided by Wuhan Anachro Technologies Co., Ltd. LC–MS analysis and chromatographic separation conditions were as follows: analysis platform: ACQUITYTM UPLC QTOF; column: XBridge™ C18 2.5 μm, 2.1 mm × 50 mm Column, Waters, USA; column temperature: 30°C; mobile phase A: 0.05% HCOOH-Water; mobile phase B: 0.05% HCOOH-CH_3CN; flow rate: 0.3 ml/min. MS parameters were as follows: for the ESI+ model, capillary voltage: 1.4 kV; sampling cone: 40 V; source temperature: 120°C; desolvation temperature: 350°C; cone gas flow: 50 L/h; desolvation gas flow: 600 L/h; collision energy: 10–40 V; ion energy: 1 V; scan time: 0.03 s; inter scan time: 0.02 s; scan range: 50–1,500 m/z. For ESI-model, capillary voltage: 1.3 kV; sampling cone: 23 V; source temperature: 120°C; desolvation temperature: 350°C; cone gas flow: 50 L/h; desolvation gas flow: 600 L/h; collision energy: 10–40 V; ion energy: 1 V; scan time: 0.03 s; inter scan time: 0.02 s; scan range: 50–1,500 m/z. Data were then normalized and edited into a two-dimensional data matrix using the Excel 2010 software, including retention time (RT), mass, observations (samples), and peak intensity.

Genomic DNA extraction, sequencing, and quantitative analysis of microbiome composition

The DNA was extracted from the small intestine contents of mice using the TIANamp Stool DNA Kit (Tiangen Biochemical Technology, Beijing, China), according to the manufacturer's recommendations. The V4 region of the 16S ribosomal RNA (rRNA) gene was analyzed by using Illumina Hiseq (Novogene Bioinformatics Technology Co., Ltd.) using the following primers: 515F (5'-GTGCCAGCMGCCGCGGTAA-3') and 806R (5'-GGACTACHVGGGTWTCTAAT-3'). Pyrosequencing reads were analyzed using the Quantitative Insights into Microbial Ecology (QIIME) software. For taxonomic assignment, sequence reads were grouped into operational taxonomic units (OTUs) at a sequence similarity level of 97%.

Protein preparation and western blot

The samples of small intestine tissue were washed three times with cold phosphate-buffered saline before being lysed in Radio Immunoprecipitation Assay (RIPA) lysis buffer containing phenylmethanesulfonyl fluoride (Beyotime Biotechnology Company, Jiangsu, China) on ice and centrifuged at 4°C, 6,000 g for 20 min. A bicinchoninic acid (BCA) protein assay kit (Beyotime Biotechnology Company, Jiangsu, China) was used to measure protein concentrations. Antibodies against CLOCK, REV-ERBα, FXR, SHP, FGF15, and β-actin were obtained from Santa Cruz Biotechnology, Inc. (Cambridge, MA, USA). Specific protein expression levels were normalized to β-actin for total protein analyses. Blots were detected using the ChemiDoc™ MP System detection system (Bio-Rad Laboratories, Inc., Hercules, CA, USA). Membranes

were scanned, and the sum optical density was quantitatively analyzed using the Image Lab software (Bio-Rad Laboratories, Inc., Ltd, Japan).

Statistical analysis

Data are presented as mean ± SD. One-way ANOVA with Tukey's post hoc analysis was conducted to determine significant differences. All analyses were performed using GraphPad Prism 8. $P < 0.05$ was considered statistically significant. Heatmap analysis of differential metabolites was performed using RStudio.

Results

Changes to lipid metabolism in Per1/Per2$^{-/-}$ *mice*

As shown in Fig. 1A, the body weight and fat/body weight ratio of DKO mice were significantly reduced compared with WT mice under the CON diet ($P < 0.01$) but without significant differences in liver/body weight ratio. Under the HFD diet, the body weight, fat/body weight ratio, and liver/body weight ratio of WT and DKO mice were all significantly increased compared with the CON diet ($P < 0.01$), with the liver/body weight ratio of DKO mice even higher than that of WT mice ($P < 0.05$), but without significant differences in body weight or fat/body weight ratio between WT and DKO mice.

The plasma TC content of DKO mice fed with a normal diet was slightly higher than that of WT mice, and the difference was significant only at ZT12 ($P < 0.05$). A high-fat diet can significantly increase TC content in DKO and WT mice, but the increase in DKO mice was greater and significantly higher than that seen in WT mice ($P < 0.01$). There was no obvious change in TG between the HFD and CON groups, but the circadian rhythm of TG changed significantly. In WT mice, plasma TG was significantly higher at ZT0 than at ZT12 ($P < 0.01$). In contrast, DKO mice showed lower plasma TG at ZT0 than at ZT12, resulting in TG content of DKO mice being significantly higher than that of WT mice at ZT12 ($P < 0.01$). As normal, in WT mice, TG levels were increasing during activity periods and decreasing during resting periods with high fat enhancement. However, DKO mice were different in that the diurnal fluctuations of TG disappeared in mice fed with a normal diet or even became higher than that of WT mice at ZT12 in mice fed with a high-fat diet, as shown in Fig. 1B. This finding seems to suggest that DKO mice experience diurnal reversal of lipid digestion, absorption, and metabolism under high-fat conditions.

The Oil red O staining of liver tissue showed that, under normal diet conditions, lipid droplets in the hepatocytes of WT mice were evenly dispersed throughout the cytoplasm. In comparison, significantly fewer droplets were observed in DKO mice, indicating that *Per1*/*Per2*$^{-/-}$ mice have reduced hepatocytic lipid content. However, under a high-fat diet, both DKO and WT mice showed tremendous cytoplasmic accumulation of lipids. H&E staining showed that the small intestine cells of WT and DKO mice showed normal morphologies in mice fed with a normal diet but were marked by swelling and deformations filled with lipid droplets of various sizes scattered throughout the cytoplasm in mice fed with a high-fat diet, and the nucleus was marginal in both mice, as shown in Fig. 1C.

Intestinal circadian rhythm changes in Per1/Per2$^{-/-}$ *mice*

The experiment further demonstrated the effect of *Per1*/*Per2* gene knockout on the circadian rhythm of the intestinal biological clock. Protein expression of the intestinal core clock molecule showed that CLOCK and REV-ERBα expressions in WT mice fluctuated between day and night, with higher expression at ZT0 than ZT12 ($P < 0.05$) regardless of diet. However, these circadian rhythm fluctuations disappeared in DKO rats fed with a normal diet, and the circadian rhythm was reversed in mice fed with a high fat (as demonstrated by the sharp increase at ZT12), as shown in Fig. 2. The rhythmic changes in the expression of intestinal clock molecules in DKO mice are related to intestinal activities and may affect both lipid absorption and fluctuations of blood triglycerides. Especially, under high-fat feeding conditions, the diurnal expression changes of the aforementioned clock molecules are consistent with diurnal changes of blood TG. Both increase significantly at ZT12, indicating that at this time, intestinal activity was enhanced, and circadian rhythm was reversed. Abnormal circadian rhythm can perturb normal digestion and absorption rhythms and influence secretory function and immune regulation function of the intestine. These effects can cause lipid metabolism disorder and intestinal function-related diseases, including constipation and intestinal stress syndrome (28–31).

Per1/Per2 *DKO mice show disrupted circadian patterns of intestinal BA content*

The quantitative results of intestinal BAs were listed in Attached Supplementary Table 2 and were divided into two categories: 1) conjugated BA, including ω-TMCA, β-TMCA, TCA, α-TMCA, TDCA, TCDCA, THDCA, GCA, GCDCA, GDCA, GHDCA, and GLCA; 2) unconjugated BAs, including β-MCA, CA, αMCA, MoCA, λ-MCA, CDCA, DCA, ALCA, 12-KLCA, 7-KDCA, HDCA, LCA, UDCA, DLCA, 3-DHCA, 6,7-DKLCA, and NDCA.

Figure 3 shows the ratios of total, unconjugated, and conjugated BA in mice colon samples.

Total BA content was drastically reduced in DKO mice compared to WT mice (about a twofold change). Under a normal diet, the total BA of WT mice at ZT0 was about twice that at ZT12 (ZT0:ZT12 = 2:1); the day/

Citation: Food & Nutrition Research 2022, **66**: 7653 - http://dx.doi.org/10.29219/fnr.v66.7653

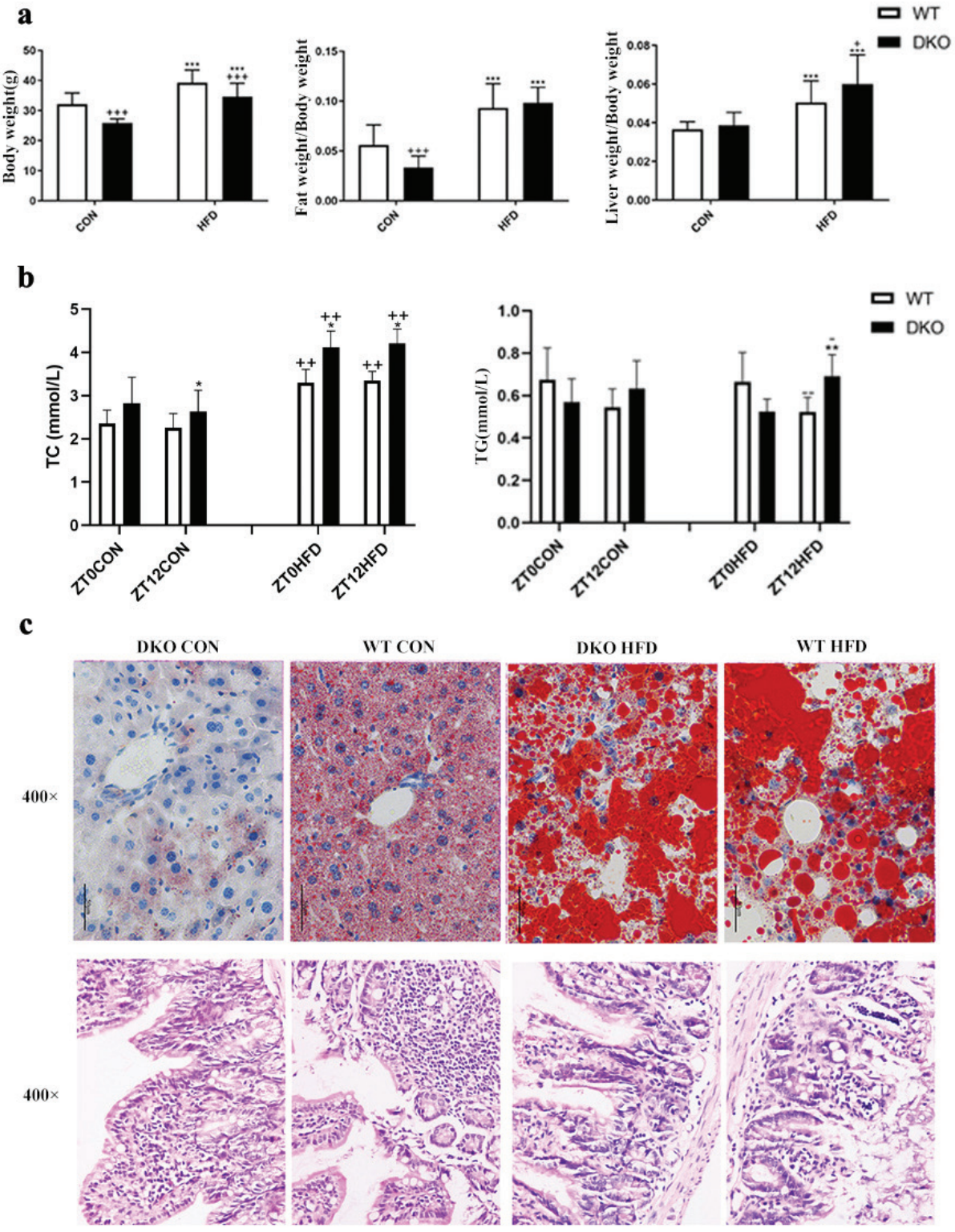

Fig. 1. Dyslipidemia induced by *Per1*/*Per2*$^{-/-}$and high-fat diet. At the end of the 16th week, body weight, fat weight/body weight ratio, and liver weight/body weight ratio (a), plasma TC, TG, HDL-C, and LDL-C (b), liver tissue Oil red O staining and intestinal tissue H&E staining (c) of each group. Data are expressed as mean ± SD (n = 10 per group). '*' is the comparison between the WT group and the DKO group, '+' is the comparison between the CON group and the HFD group, and '-' is the comparison between the ZT0 group and the ZT12 group; *, +, - $P < 0.05$; **, ++, -- $P < 0.01$; ***, +++, --- $P < 0.001$.

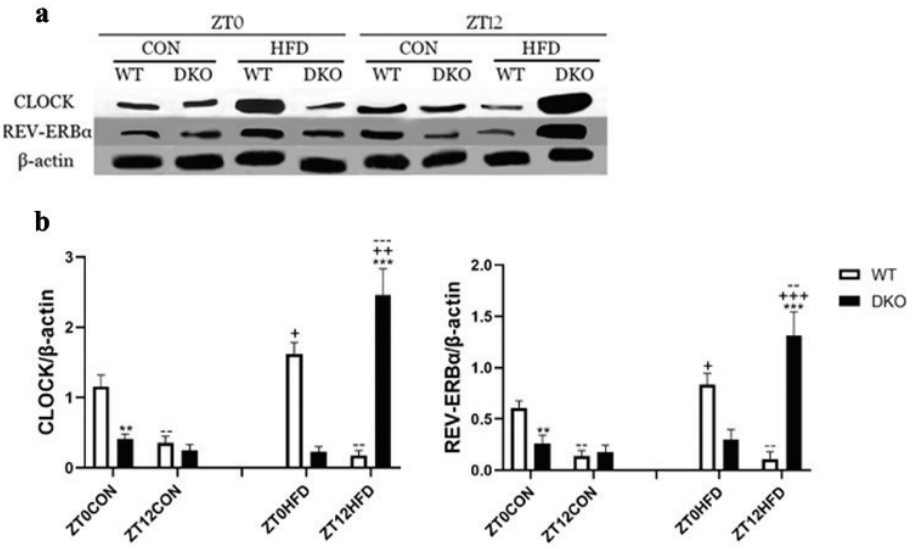

Fig. 2. Circadian changes to intestinal expression of CLOCK and REV-ERBα. Expression of CLOCK and REV-ERBα proteins in small intestine tissues of mice was measured by western blot and gray scale analyses (a and b). Data are expressed as mean ± SD (n = 3 per group). '*' is the comparison between the WT group and the DKO group, and '+' is the comparison between the CON group and the HFD group. *,+,-P < 0.05; **,++,--P < 0.01; ***, +++,---P < 0.001.

night ratio was about 1:1 in DKO mice (ZT0:ZT12 = 1:1). High-fat feeding caused a conspicuous increase in both DKO and WT mice, about 1.7-2 times that of a normal diet. However, WT mice still maintain a ratio nearly twice higher at ZT0 than at ZT12, while DKO mice maintained roughly the same day/night ratio (1:1). This finding demonstrates a clear circadian rhythm in total BA for WT mice (ZT0:ZT12 = 2:1), which became adapted to circadian activities and eating habits. However, upon knockout of key rhythm genes in DKO mice, the circadian fluctuation in total BAs disappeared, regardless of diet, as shown in Fig. 3A. Of note, because of the reduction of total BA seen in DKO mice, their digestion, absorption, and metabolism functions were affected, thereby affecting their growth. This may explain why DKO mice were thinner than WT mice when fed with a normal diet.

The content of conjugated BA in WT mice was significantly higher than in DKO mice at both day and night, irrespective of diet. Notably, the content of conjugated BA in WT mice was five times that of DKO mice at ZT0,but was lowered to about two times that of DKO mice at ZT12. In terms of circadian rhythm, the content of conjugated BA in WT mice was remarkably increased at ZT0 compared to ZT12, with a four- to five-fold difference consistent with a 'night-high, day-low' pattern. The content of conjugated BA in DKO mice was almost the same at ZT0 and ZT12, as shown in Fig. 3B. These results showed that the circadian rhythm of conjugated BA in WT mice was obvious and was related to mice more eating during their nocturnal period and less during their rest period. However, this rhythm (proportion of day and night) had nothing to do with diet. The disappearance of this circadian rhythm in DKO mice indicated that there were no differences between the mice's eating activities between day and night. Conjugated BA was the main type of BA synthesized and secreted by the liver, and it plays a major role in the digestion and absorption of lipid food. The significant decrease in conjugated BAs observed in DKO mice indicates that *Per1*/*Per2*$^{-/-}$ leads to a conspicuous decrease in liver BAs synthesis as well as in intestinal lipid digestion and absorption.

Unconjugated BA content in WT mice was still significantly higher than in DKO mice. However, the diurnal changes of WT or DKO mice were not obvious under normal or high-fat diets (only the high-fat feeding WT mice showed a slight decrease at ZT12). The high-fat diet could significantly increase unconjugated BA content in both DKO and WT mice to about twice that of the normal diet, as shown in Fig. 3C. This experiment also demonstrated that the total amount of unconjugated BA remained relatively stable between day and night, with an inconspicuous circadian rhythm but can be significantly increased by a high-fat diet. Since unconjugated BA in the colon was mainly produced by the metabolism of conjugated BA via intestinal microorganisms, and conjugated BA showed obvious circadian rhythms, the unsynchronized circadian relationship between unconjugated and conjugated BAs suggests that the intestinal bacterial

Citation: Food & Nutrition Research 2022, **66**: 7653 - http://dx.doi.org/10.29219/fnr.v66.7653

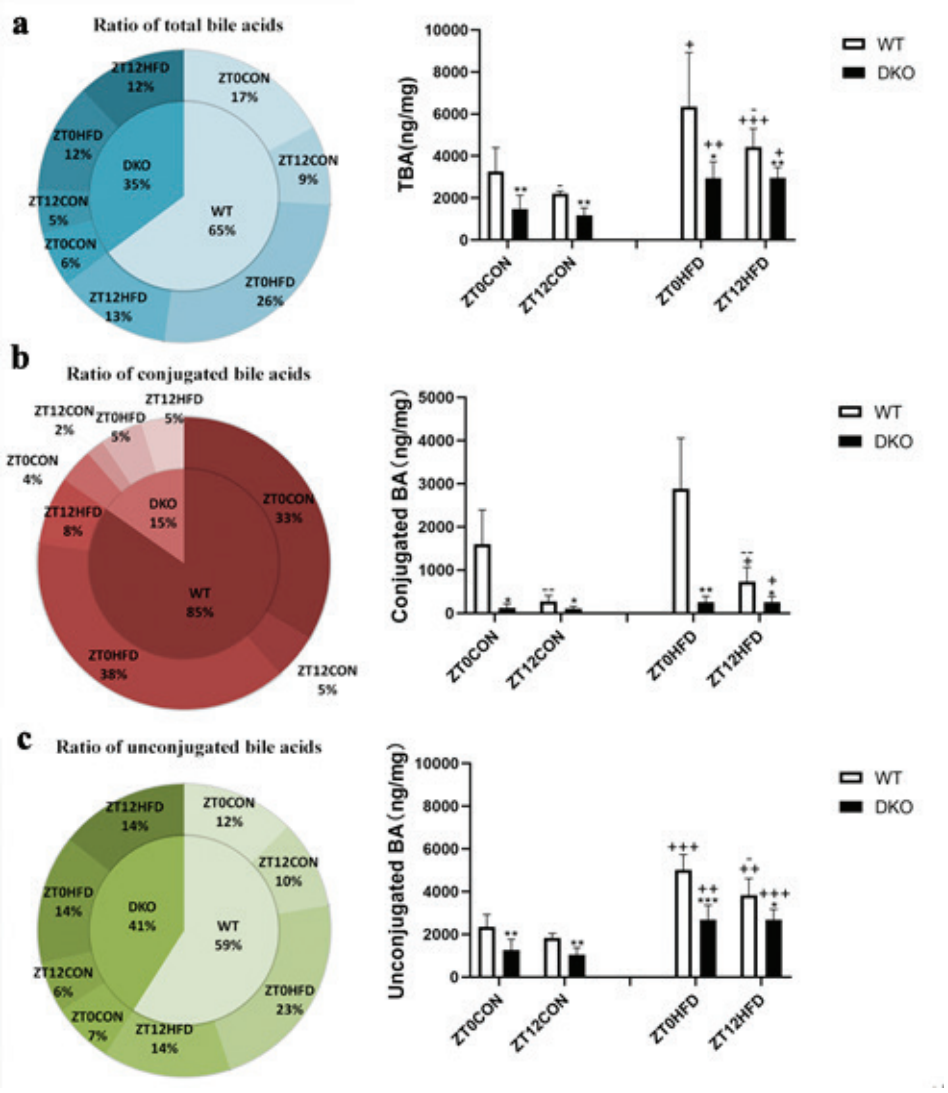

Fig. 3. *Per1*/*Per2* DKO mice show altered bile acid expression patterns. The ratio of intestinal total (a), conjugated (b), and unconjugated (c) bile acids in mice in each group. The proportion of each group in the pie chart = the content of bile acid in this group/total bile acid (conjugated bile acid/unconjugated bile acid). Data are expressed as mean ± SD (n = 6 per group). '*' is the comparison between the WT group and the DKO group, '+' is the comparison between the CON group and the HFD group, and '-' is the comparison between the ZT0 group and the ZT12 group. *,+,-$P < 0.05$; **,++,--$P < 0.01$; ***,+++,---$P < 0.001$.

involved in BA metabolism might be relatively stable between day and night.

Circadian relationship between small intestinal BA metabolism and flora abundance

Within the mouse small intestine, conjugated BA is broken down into unconjugated BA through the action of intestinal flora. Therefore, we correlated intestinal BA metabolism with the abundance of small intestinal flora, as detected by 16srRNA gene sequencing (Attached Supplementary Table 3). These results showed that the abundance of most intestinal flora was positively correlated with levels of conjugated BA, including *Deferribacteres*, *Fusobacteria*, *Tenericutes*, *Actinobacteria*, *Candidatus*, *Saccharibacteria*, *Proteobacteria*, and *Bacteroidetes*. In particular, *Fusobacteria* and *Bacteroidetes* were significantly positively correlated with the content of conjugated BA ω-TMCA ($P < 0.05$), indicating that these phyla have become adapted to the high conjugated bile acid content of the lipid digestion environment. In contrast, *Firmicutes* seemed to be significantly negatively correlated with the conjugated BA TCDCA ($P < 0.05$)

and positively correlated to unconjugated BAs such as 12-KLCA, DCA, DLCA, and NDCA. These findings suggest that *Firmicutes* and *Bacteroidetes* might participate in the process by which conjugated BA is metabolized into unconjugated BAs, as shown in Fig. 4. Although *Proteobateria* and NDCA are also significantly negatively correlated, NDCA content is too low, and the analysis is of little significance.

According to the correlation analysis shown in Fig. 4, *Bacteroides* was positively correlated with conjugated bile acids and negatively correlated with unconjugated bile acids. Further analysis of the role that *Bacteroides* plays in bile acid metabolism, as well as into its own diurnal changes, showed that the abundance of *Bacteroidetes* in WT mice fluctuated considerably (levels at ZT0 were much higher than at ZT12). This result was consistent with the ratio of conjugated bile acid/total bile acid and opposite to the ratios of unconjugated bile acid/total bile acid and unconjugated bile acid/conjugated bile acid (ZT0 was much lower than ZT12). Nevertheless, for WT mice, the abundance of *Firmicutes* fluctuated in opposition to abundance of *Bacteroides*, such that it was consistent with the ratio of unconjugated BA/conjugated BA and was opposite to the ratio of conjugated BA/total BA. In the small intestines of DKO mice, diurnal fluctuations in the abundance of *Bacteroidetes*, *Firmicutes*, intestinal unconjugated bile acid/total bile acid, conjugated bile acid/total bile acid, and unconjugated bile acid/conjugated bile acid ratio were abolished (Fig. 5A).

Two representative conjugated bile acids and unconjugated bile acids were selected for analysis, and their changes in each group are shown in Fig. 5B. The TCA content of WT mice was significantly higher than that of DKO mice regardless of daytime and nighttime diets ($P < 0.01$). High-fat diet significantly increased TCA content in WT mice at ZT0 ($P < 0.01$), while TCA content at ZT12 was not affected by high-fat diet. Similarly, βTMCA was higher in WT mice than in DKO mice regardless of diet at day or night, but with obvious diurnal differences (higher ZT12 than ZT0) seen for HFD mice. DCA content of WT mice was significantly higher than that of DKO mice regardless of diet during both day and night ($P < 0.05$). High-fat diet significantly increased DCA content in DKO mice ($P < 0.01$) without day- or night-related changes. With regard to LCA, levels were significantly higher in WT mice than in DKO mice fed with a normal diet. The high-fat diet significantly increased their contents in DKO mice. Comprehensively, the varieties of these four bile acids observed in each group were basically similar to those seen for conjugated and unconjugated bile acids, indicating that bile acids are generally stable in the small intestine.

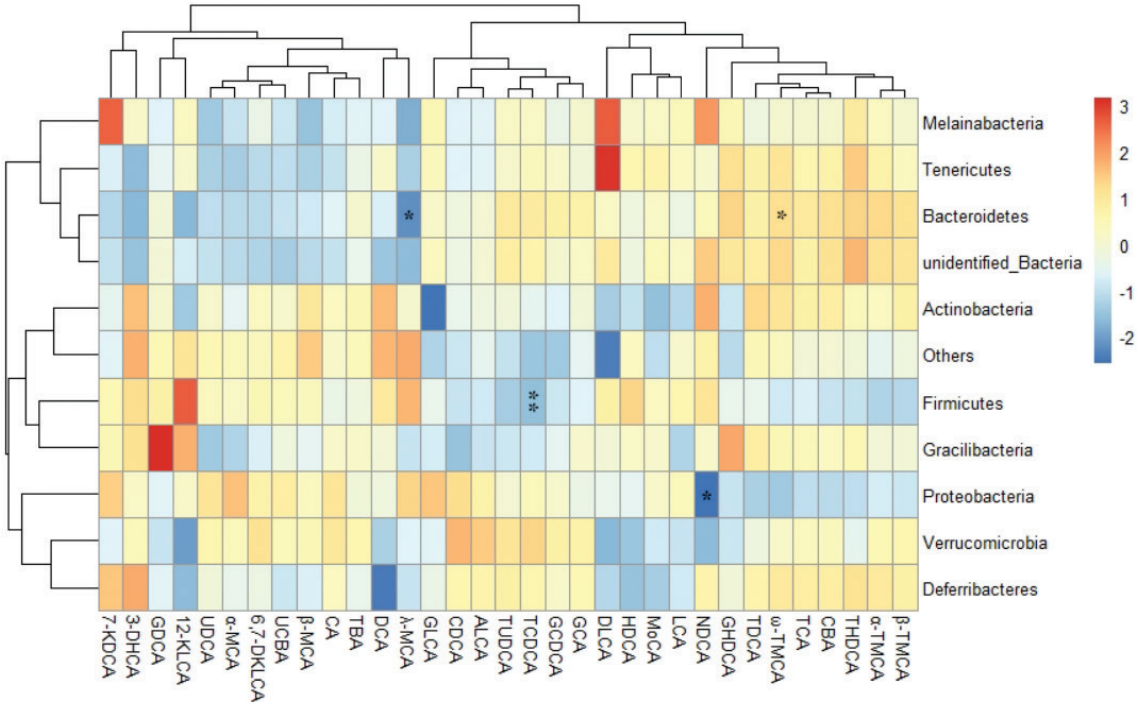

Fig. 4. Correlation analysis of BA content and phylum. Heatmap of intestinal BAs and flora phylum. RStudio was used to draw the heatmap, Data are expressed as mean ± SD ($n = 6$ per group). '*' is the comparison between BA and phylum. * $P < 0.05$; ** $P < 0.01$.

Citation: Food & Nutrition Research 2022, **66**: 7653 - http://dx.doi.org/10.29219/fnr.v66.7653

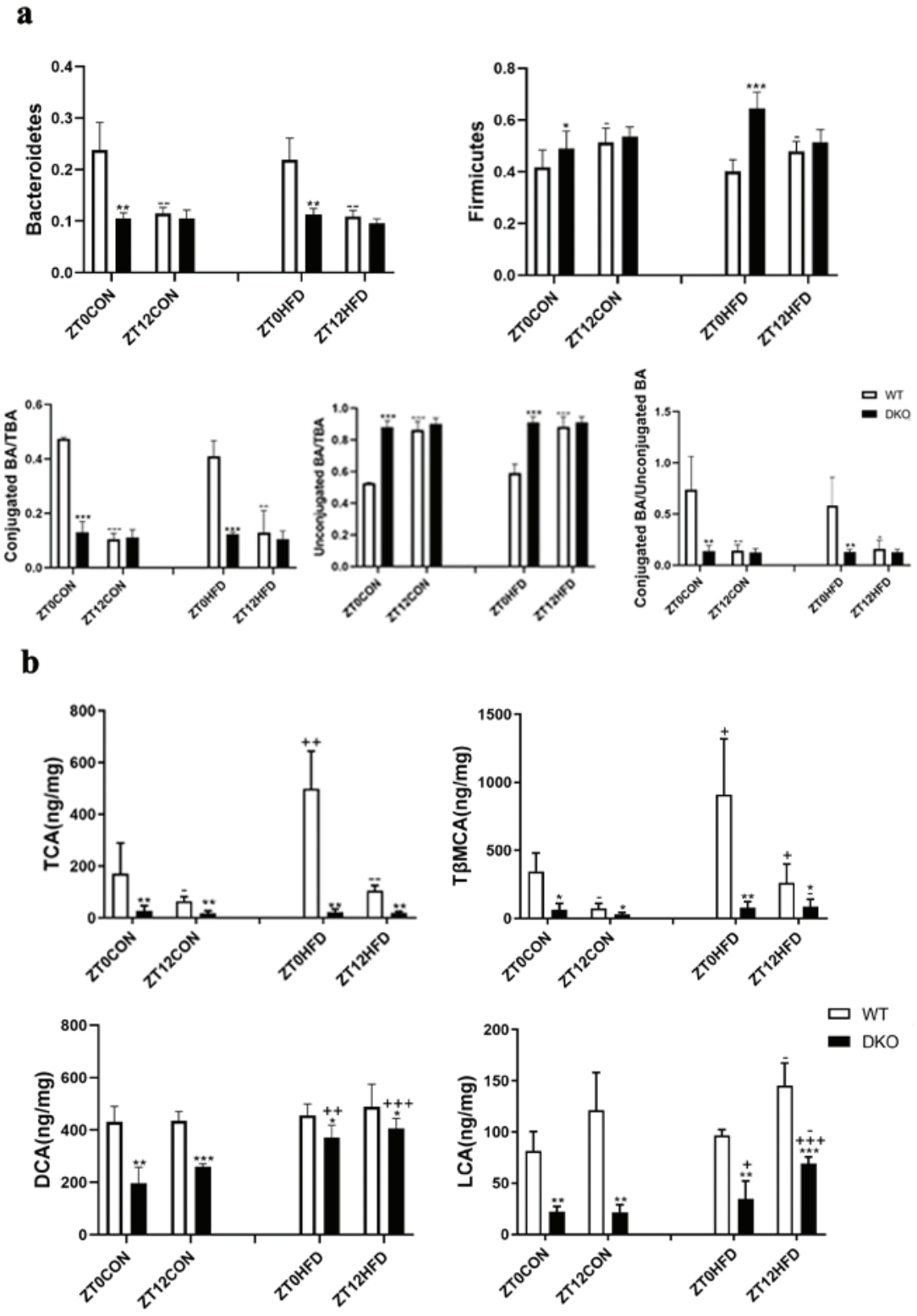

Fig. 5. *Per1*/*Per2*$^{-/-}$ mice show changes in diurnal expression patterns of bile acids in the small intestine. Abundance of *Bacteroidetes*, *Firmicutes*, conjugated bile acid, and unconjugated bile acid (a) and DCA, ALCA, 12-KLCA, and LCA (b) in each group of mice. Data are expressed as mean ± SD (n = 12 per group). '*' is the comparison between the WT group and the DKO group, '+' is the comparison between the CON group and the HFD group, and '-' is the comparison between the ZT0 group and the ZT12 group. *,+,- $P < 0.05$; **, ++,-- $P < 0.01$; ***,+++,---$P < 0.001$.

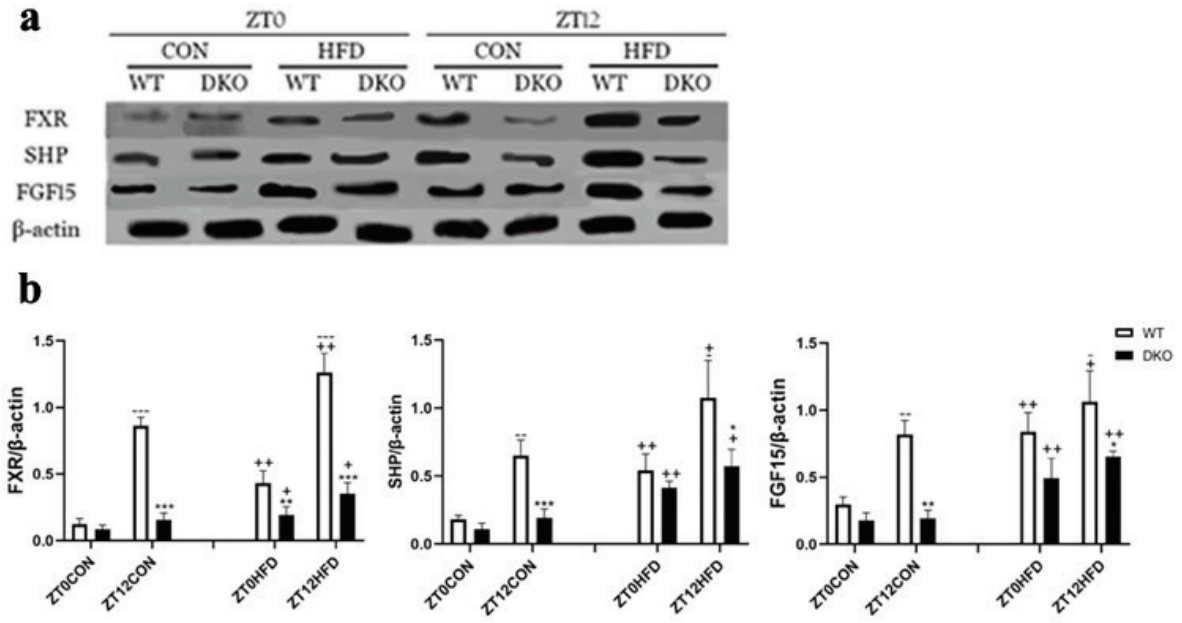

Fig. 6. Diurnal expression of intestinal BA regulatory proteins. Protein expression levels of FXR, SHP, and FGF15 in the small intestine tissue of mice were measured by western blot and gray scale analysis (a and b). Data are expressed as mean ± SD ($n = 3$ per group). '*' is the comparison between the WT group and the DKO group, '+' is the comparison between the CON group and the HFD group. *,+,- $P < 0.05$; **,++,-- $P < 0.01$; ***,+++,---$P < 0.001$.

In Per1/Per2$^{-/-}$ *mice, the circadian rhythm of hepatic bile acid synthesis is regulated through intestinal bile acid receptor FXR signal*

FXR, SHP, and the hormone signal FGF15 are key proteins involved in intestinal bile acid metabolism. Their expression trends were essentially the same in both WT and DKO mice. SHP, for example, was expressed at significantly lower levels in DKO mice than in WT mice, which has been linked to the lower BA levels of DKO mice compared to WT mice. With regard to circadian rhythm, the expression of WT mice at ZT12 was substantially higher than at ZT0 (about two- to three-fold), while differences between day and night were abolished in DKO mice. High-fat diet significantly increased the expression of SHP (1.6-3 times higher than normal diet). In short, in DKO mice, BA receptor FXR pathway signal was weakened without circadian rhythm, and a high-fat diet can sharply increase intestinal expression of SHP and FGF15.

The experimental results showed that FGF15 expression was higher at ZT12 (reflecting the resting period of mice), thus inhibiting liver BA synthesis. This finding was in agreement with that of lower conjugated BA content at ZT12 compared to ZT0. Under a high-fat diet, although the BA synthesis promoted by dietary factors was significantly enhanced, the expression of FGF15 still followed a circadian rhythm and was higher at ZT12 than that at ZT0.

Discussion

In WT mice, intestinal total BA and conjugated BA displayed circadian rhythm changes that were adapted to mice circadian activities and eating habits, which disappeared in DKO mice. The content of unconjugated BAs did not change significantly between day and night in either WT or DKO mice under both normal and high-fat diets. Since unconjugated BA is produced by intestinal flora through metabolism of conjugated BA, the loss of circadian rhythm in unconjugated BA levels indicates that the circadian abundance of flora involved in intestinal BA metabolism is relatively stable. Our results with respect to the relative abundance of mouse intestinal flora confirmed this pattern.

Studies have shown that intestinal flora, such as Clostridium, Lactobacillus, Clostridiales, Enterococcus, Eubacterium, Bifidobacterium, and Bacteroides, can deconjugate conjugated BAs and oxidize or isomerize to produce both unconjugated BAs and secondary BAs (14, 32–33). As for Bacteroidetes, some literature has suggested that the increased abundance of Bacteroidetes reduces the content of intestinal conjugated bile acids and raises the content of unconjugated bile acids (34). However, other reports have shown that Bacteroidetes is negatively correlated with the content of unconjugated bile acid (35). Our correlation analysis showed that diurnal fluctuations in *Bacteroidetes*, which have already been shown to be involved in the metabolic transformation of conjugated

Citation: Food & Nutrition Research 2022, **66**: 7653 - http://dx.doi.org/10.29219/fnr.v66.7653

BAs (36), appeared to be related to circadian changes in conjugated BA/unconjugated BA. These levels showed obvious diurnal fluctuations in WT mice, which were consistent with circadian fluctuations of conjugated BA and contrary to those of unconjugated BAs. However, these diurnal fluctuations of *Bacteroidetes* and conjugated BA/unconjugated BA disappeared in DKO mice. Our results demonstrate the important rhythmic characteristics of intestinal BA metabolism and suggest that conjugated and unconjugated BAs might play different roles in lipid absorption and metabolism. Conjugated BA, secreting from the liver into the intestine, acts as an emulsifier to promote digestion and lipid absorption. Unconjugated BAs are primarily involved in the regulation of intestinal metabolism, including stimulating expression of BA receptor proteins FXR and TGR5 (37, 38) and participating in intestinal lipid metabolism (39), glucose metabolism (40), and the regulation of liver BA synthesis (41).

In the FXR pathway, SHP activates the expressed endocrine factor FGF15 (42), which is secreted from the intestine into the blood and taken up by the liver receptor Fibroblast growth factor receptor 4 (FGFR4). FGFR4 can inhibit the expression of the key BA synthesis enzyme cholesterol 7a-hydroxylase (CYP7A1), thereby reducing BA synthesis in the liver. Intestinal expression of FXR signal in WT mice (including SHP and FGF15 proteins) was significantly reduced in the active phase (ZT0), related to the high ratio of conjugated BA/unconjugated BA observed at the same time. In contrast, the diurnal fluctuations of this signal pathway disappeared in DKO mice, mirroring changes in the ratio of conjugated/unconjugated BA. On the other hand, the expression of FXR signal was significantly higher in mice fed with a high-fat diet than those fed with a normal diet ($P < 0.05$) for both WT and DKO mice, suggesting that a high-fat diet can upregulate the expression of FXR signal. Intestinal FXR signal can regulate lipid metabolism by reducing plasma TG, fatty acids, and cholesterol (40), affect glucose metabolism by improving insulin sensitivity and inhibiting hepatic gluconeogenesis (41) via FGF15 release and uptake by the liver to inhibit BA synthesis, and protect the liver from cholestasis (43). Our study found that diurnal fluctuations in the FXR signaling pathway are related to the ratio of conjugated/unconjugated BA. In *Per1*/*Per2* knockout mice, diurnal fluctuations of the FXR signaling pathway disappeared, disrupting intestinal glucose and lipid metabolism and liver BA anabolism. Otherwise, factors such as diet seem to have a greater role than previously appreciated in the regulation of total BA.

Intestinal circadian rhythm is affected by factors such as the central nervous system, diet, and intestinal flora (44). Our results showed that in WT mice, intestinal expression of CLOCK and REV-ERBα shows an obvious circadian rhythm (ZT0 higher than ZT12) under normal or high-fat diets. However, DKO mice show completely different patterns; circadian rhythm disappears under a normal diet, and circadian rhythm is reversed under a high-fat diet. These results suggest that the circadian clock plays a key role in maintaining intestinal circadian rhythm. Knockout of *Per1*/*Per2* genes can cause disappearance of circadian fluctuations and disorder of circadian rhythm, and inevitably affecting intestinal lipid metabolism (45), hormone secretion (30), and immune regulation (46).

In short, the circadian rhythms of different types of BAs in the intestine are significantly different, and their levels are both controlled by the circadian clock and affected by a high-fat diet. Under both normal and high-fat diets, WT mice exhibit obvious circadian rhythms in levels of conjugated BAs, while levels of unconjugated BAs remain relatively stable between day and night. The low BA content and disappearing circadian rhythm in DKO mice are important reasons for their low body weights. This study shows that diurnal changes in intestinal ratios of conjugated BA/unconjugated BA, which are related to diurnal fluctuations in *Bacteroidetes* abundance, can regulate diurnal fluctuations of liver BA synthesis through the BA receptor pathway FXR-SHP-FGF15. The inverted circadian rhythm observed in the intestinal circadian clocks of DKO mice under a high-fat diet may be an important reason for their sensitivity to lipid metabolism disorders.

Authors' contributions

The corresponding author affirms that all listed authors meet authorship criteria, and that no others meeting these criteria have been omitted.

Acknowledgments

This study was supported by the National Natural Science Foundation of China (Grant No. 31271855), the Thirteen-Fifth Mega-Scientific Project (Grant No. 2017ZX10201301-003-003), Wuhan Science and Technology Project (Grant No. 2018020402011230), and the central government guides local science and technology development projects (Grant No. 2019ZYYD).

Conflicts of interest and funding

The authors declare no conflict of interest.

References

1. Hastings MH, Smyllie NJ, Patton AP. Molecular-genetic manipulation of the suprachiasmatic nucleus circadian clock. J Mol Biol 2020. 432(12): 3639–3660. doi: 10.1016/j.jmb.2020.01.019
2. Shi D, Chen J, Wang J, Yao J, Huang Y, Zhang G, et al. Circadian clock genes in the metabolism of non-alcoholic fatty liver disease. Front Physiol 2019; 10: 423. doi: 10.3389/fphys.2019.00423
3. Figueroa AL, Figueiredo H, Rebuffat SA, Vieira E, Gomis R. Taurine treatment modulates circadian rhythms in mice fed a high fat diet. Sci Rep 2016; 6: 36801. doi: 10.1038/srep36801

4. Koga Y, Tsurumaki H, Aoki-Saito H, Sato M, Yatomi M, Takehara K, et al. Roles of cyclic AMP response element binding activation in the ERK1/2 and p38 MAPK signalling pathway in central nervous system, cardiovascular system, osteoclast differentiation and mucin and cytokine production. Int J Mol Sci 2019; 20(6): 1346. doi: 10.3390/ijms20061346
5. Lin R, Mo Y, Zha H, Qu Z, Xie P, Zhu ZJ, et al. CLOCK acetylates ASS1 to drive circadian rhythm of ureagenesis. Mol Cell 2017; 68: 198–209. doi: 10.1016/j.molcel.2017.09.008
6. Eng G, Edison, Virshup DM. Site-specific phosphorylation of casein kinase 1 delta (CK1delta) regulates its activity towards the circadian regulator PER2. PLoS One 2017; 12: e177834. doi: 10.1371/journal.pone.0177834
7. Brown AJ, Pendergast JS, Yamazaki S. Peripheral circadian oscillators. Yale J Biol Med 2019; 92: 327–35.
8. Ikeda R, Tsuchiya Y, Koike N, Umemura Y, Inokawa H, Ono R, et al. REV-ERBalpha and REV-ERBbeta function as key factors regulating mammalian circadian output. Sci Rep 2019; 9: 10171. doi: 10.1038/s41598-019-46656-0
9. Li Y, Ma J, Yao K, Su W, Tan B, Wu X, et al. Circadian rhythms and obesity: timekeeping governs lipid metabolism. J Pineal Res 2020; 69(3): e12682. doi: 10.1111/jpi.12682
10. Chen R, Zuo Z, Li Q, Wang H, Li N, Zhang H, et al. DHA substitution overcomes high-fat diet-induced disturbance in the circadian rhythm of lipid metabolism. Food Funct 2020; 11: 3621–3631. doi: 10.1039/C9FO02606A
11. Zhang L, Yan R, Wu Z. Metagenomics analysis of intestinal flora modulatory effect of green tea polyphenols by a circadian rhythm dysfunction mouse model. J Food Biochem 2020: 44(10): e13430. e13430. doi: 10.1111/jfbc.13430
12. Koh A, De Vadder F, Kovatcheva-Datchary P, Backhed F. From dietary fiber to host physiology: short-chain fatty acids as key bacterial metabolites. Cell 2016; 165: 1332–45. doi: 10.1016/j.cell.2016.05.041
13. Guan D, Xiong Y, Borck PC, Jang C, Doulias PT, Papazyan R, et al. Diet-induced circadian enhancer remodeling synchronizes opposing hepatic lipid metabolic processes. Cell 2018; 174: 831–42. doi: 10.1016/j.cell.2018.06.031
14. Doden H, Sallam LA, Devendran S, Ly L, Doden G, Daniel SL, et al. Metabolism of oxo-bile acids and characterization of recombinant 12alpha-hydroxysteroid dehydrogenases from bile acid 7alpha-dehydroxylating human gut bacteria. Appl Environ Microbiol 2018; 84(10): e00235–18. doi: 10.1128/AEM.00235-18
15. Rodriguez-Antonio I, Lopez-Sanchez GN, Garrido-Camacho VY, Uribe M, Chavez-Tapia NC, Nuno-Lambarri N. Cholecystectomy as a risk factor for non-alcoholic fatty liver disease development. HPB 2020; 22(11): 1513–1520. doi: 10.1016/j.hpb.2020.07.011
16. Di Ciaula A, Garruti G, Lunardi BR, Molina-Molina E, Bonfrate L, Wang DQ, et al. Bile acid physiology. Ann Hepatol 2017; 16: s4–14. doi: 10.5604/01.3001.0010.5493
17. Lee SM, Kim N, Yoon H, Kim YS, Choi SI, Park JH, et al. Compositional and functional changes in the gut microbiota in irritable bowel syndrome patients. Gut Liver 2021; 15(2): 253–261. doi: 10.5009/gnl19379
18. Liu Y, Li Q, Wang H, Zhao X, Li N, Zhang H, et al. Fish oil alleviates circadian bile composition dysregulation in male mice with NAFLD. J Nutr Biochem 2019; 69: 53–62. doi: 10.1016/j.jnutbio.2019.03.005
19. Gui L, Chen S, Wang H, Ruan M, Liu Y, Li N, et al. omega-3 PUFAs alleviate high-fat diet-induced circadian intestinal microbes dysbiosis. Mol Nutr Food Res 2019; 63: e1900492. doi: 10.1002/mnfr.201900492
20. Qiang S, Tao L, Zhou J, Wang Q, Wang K, Lu M, et al. Knockout of farnesoid X receptor aggravates process of diabetic cardiomyopathy. Diabetes Res Clin Pract 2020; 161: 108033. doi: 10.1016/j.diabres.2020.108033
21. Byun S, Jung H, Chen J, Kim YC, Kim DH, Kong B, et al. Phosphorylation of hepatic farnesoid X receptor by FGF19 signaling-activated Src maintains cholesterol levels and protects from atherosclerosis. J Biol Chem 2019; 294: 8732–44. doi: 10.1074/jbc.RA119.008360
22. Schumacher JD, Guo GL. Pharmacologic modulation of bile acid-FXR-FGF15/FGF19 pathway for the treatment of nonalcoholic steatohepatitis. Handb Exp Pharmacol 2019; 256: 325–57. doi: 10.1007/164_2019_228
23. Nohara K, Nemkov T, D'Alessandro A, Yoo SH, Chen Z. Coordinate regulation of cholesterol and bile acid metabolism by the clock modifier nobiletin in metabolically challenged old mice. Int J Mol Sci 2019; 20(17): 4281. doi: 10.3390/ijms20174281
24. Li WK, Li H, Lu YF, Li YY, Fu ZD, Liu J. Atorvastatin alters the expression of genes related to bile acid metabolism and circadian clock in livers of mice. PeerJ 2017; 5: e3348. doi: 10.7717/peerj.3348
25. Dabke K, Hendrick G, Devkota S. The gut microbiome and metabolic syndrome. J Clin Invest 2019; 129: 4050–7. doi: 10.1172/JCI129194
26. Ma K, Xiao R, Tseng HT, Shan L, Fu L, Moore DD. Circadian dysregulation disrupts bile acid homeostasis. PLoS One 2009; 4: e6843. doi: 10.1371/journal.pone.0006843
27. Zheng UB, Albrecht K, Kaasik M, Sage W, Lu S, Vaishnav Q, et al. Nonredundant roles of the mPer1 and mPer2 genes in the mammalian circadian clock. Cell 2001; 105(5): 683–94. doi: 10.1016/S0092-8674(01)00380-4
28. Xu L, Wu T, Li H, Ni Y, Fu Z. An individual 12-h shift of the light-dark cycle alters the pancreatic and duodenal circadian rhythm and digestive function. Acta Biochim Biophys Sinica 2017; 49(10): 954–61. doi: 10.1093/abbs/gmx084
29. Voigt RM, Forsyth CB, Keshavarzian A. Circadian rhythms: a regulator of gastrointestinal health and dysfunction. Expert Rev Gastroenterol Hepatol 2019; 13: 411–24. doi: 10.1080/17474124.2019.1595588
30. Duboc H, Coffin B, Siproudhis L. Disruption of circadian rhythms and gut motility: an overview of underlying mechanisms and associated pathologies. J Clin Gastroenterol 2020; 54: 405–14. doi: 10.1097/MCG.0000000000001333
31. Oster H, Challet E, Ott V, Arvat E, de Kloet ER, Dijk DJ, et al. The functional and clinical significance of the 24-hour rhythm of circulating glucocorticoids. Endocr Rev 2017; 38: 3–45. doi: 10.1210/er.2015-1080
32. Kriaa A, Bourgin M, Potiron A, Mkaouar H, Jablaoui A, Gerard P, et al. Microbial impact on cholesterol and bile acid metabolism: current status and future prospects. J Lipid Res 2019; 60: 323–32. doi: 10.1194/jlr.R088989
33. van Zutphen T, Stroeve J, Yang J, Bloks VW, Jurdzinski A, Roelofsen H, et al. FXR overexpression alters adipose tissue architecture in mice and limits its storage capacity leading to metabolic derangements. J Lipid Res 2019; 60(9): 1547–1561. doi: 10.1194/jlr.M094508
34. Ovadia AC, Perdones-Montero K, Spagou A, Smith MH, Sarafian M, Gomez-Romero E, et al. Enhanced microbial bile acid deconjugation and impaired ileal uptake in pregnancy repress intestinal regulation of bile acid synthesis. Hepatology 2019; 70(1): 276–93. doi: 10.1002/hep.30661

35. Zhu Y, Zhang JY, Wei YL, Hao JY, Lei YQ, Zhao WB, et al. The polyphenol-rich extract from chokeberry (Aronia melanocarpa L.) modulates gut microbiota and improves lipid metabolism in diet-induced obese rats. Nutr Metab (Lond) 2020; 17: 54. doi: 10.1186/s12986-020-00473-9
36. Ridlon JM, Harris SC, Bhowmik S, Kang DJ, Hylemon PB. Consequences of bile salt biotransformations by intestinal bacteria. Gut Microbes 2016; 7: 22–39. doi: 10.1080/19490976.2015.1127483
37. Copple BL, Li T. Pharmacology of bile acid receptors: evolution of bile acids from simple detergents to complex signaling molecules. Pharmacol Res 2016; 104: 9–21. doi: 10.1016/j.phrs.2015.12.007
38. Li T, Chiang J. Bile acid-based therapies for non-alcoholic steatohepatitis and alcoholic liver disease. Hepatobiliary Surg Nutr 2020; 9: 152–69. doi: 10.21037/hbsn.2019.09.03
39. Kumari A, Pal PD, Asthana S. Bile acids mediated potential functional interaction between FXR and FATP5 in the regulation of Lipid Metabolism. Int J Biol Sci 2020; 16(13): 2308–22. doi: 10.7150/ijbs.44774
40. Li L, Zhao H, Chen B, Fan Z, Li N, Yue J, et al. FXR activation alleviates tacrolimus-induced post-transplant diabetes mellitus by regulating renal gluconeogenesis and glucose uptake. J Transl Med 2019; 17: 418. doi: 10.1186/s12967-019-02170-5
41. Matsubara T, Li F, Gonzalez FJ. FXR signaling in the enterohepatic system. Mol Cell Endocrinol 2013; 368: 17–29. doi: 10.1016/j.mce.2012.05.004
42. Li C, Zhang XL, Xue YX, Cheng DJ, Yan JT, Wu S, et al. [Protective effect and regulating effect on FXR/SHP gene of electroacupuncture preconditioning on myocardial ischemia-reperfusion injury in rats]. Zhongguo Zhen Jiu 2019; 39: 861–6.
43. Pathak P, Xie C, Nichols RG, Ferrell JM, Boehme S, Krausz KW, et al. Intestine farnesoid X receptor agonist and the gut microbiota activate G-protein bile acid receptor-1 signaling to improve metabolism. Hepatology 2018; 68: 1574–88. doi: 10.1002/hep.29857
44. Parasram K, Bernardon N, Hammoud M, Chang H, He L, Perrimon N, et al. Intestinal stem cells exhibit conditional circadian clock function. Stem Cell Reports 2018; 11: 1287–301. doi: 10.1016/j.stemcr.2018.10.010
45. Hong F, Pan S, Xu P, Xue T, Wang J, Guo Y, et al. Melatonin orchestrates lipid homeostasis through the hepatointestinal circadian clock and microbiota during constant light exposure. Cells 2020; 9(2): 489. doi: 10.3390/cells9020489
46. Haspel JA, Anafi R, Brown MK, Cermakian N, Depner C, Desplats P, et al. Perfect timing: circadian rhythms, sleep, and immunity – an NIH workshop summary. JCI Insight 2020; 5(1): e131487. doi: 10.1172/jci.insight.131487

***Zhiguo Liu**
Hubei Province Engineering Research Center of Healthy Food
School of Biology and Pharmaceutical Engineering
Wuhan Polytechnic University
Wuhan 430023, China
Tel.:+86-27-83956899
Email: zhiguo_l@126.com